Cutting Edge: Retrobulbar Inflammation, Adipogenesis, and Acute Orbital Congestion in a Preclinical Female Mouse Model of Graves' Orbitopathy Induced by Thyrotropin Receptor Plasmid-in Vivo Electroporation

Sajad Moshkelgosha, Po-Wah So, Neil Deasy, Salvador Diaz-Cano, and J Paul Banga

Division of Diabetes and Nutritional Sciences (S.M., J.P.B.), King's College London School of Medicine; London, United Kingdom SE5 9NU; Preclinical Imaging Unit (P.-W.S.), Department of Neuroimaging, Department of Neuroradiology (N.D.), Institute of Psychiatry, King's College London, London, United Kingdom SE5 9NU; and King's College Hospital NHS Trust (S.D.-C.), Department of Pathology, London, United Kingdom SE5 9RS

Graves' orbitopathy (GO) is a complication in Graves' disease (GD) but mechanistic insights into pathogenesis remain unresolved, hampered by lack of animal model. The TSH receptor (TSHR) and perhaps IGF-1 receptor (IGF-1R) are considered relevant antigens. We show that genetic immunization of human TSHR (hTSHR) A-subunit plasmid leads to extensive remodeling of orbital tissue, recapitulating GO. Female BALB/c mice immunized with hTSHR A-subunit or control plasmids by in vivo muscle electroporation were evaluated for orbital remodeling by histopathology and magnetic resonance imaging (MRI). Antibodies to TSHR and IGF-1R were present in animals challenged with hTSHR A-subunit plasmid, with predominantly TSH blocking antibodies and were profoundly hypothyroid. Orbital pathology was characterized by interstitial inflammation of extraocular muscles with CD3+ T cells, F4/80+ macrophages, and mast cells, accompanied by glycosaminoglycan deposition with resultant separation of individual muscle fibers. Some animals showed heterogeneity in orbital pathology with 1) large infiltrate surrounding the optic nerve or 2) extensive adipogenesis with expansion of retrobulbar adipose tissue. A striking finding that underpins the new model were the in vivo MRI scans of mouse orbital region that provided clear and quantifiable evidence of orbital muscle hypertrophy with protrusion (proptosis) of the eye. Additionally, eyelid manifestations of chemosis, including dilated and congested orbital blood vessels, were visually apparent. Immunization with control plasmids failed to show any orbital pathology. Overall, these findings support TSHR as the pathogenic antigen in GO. Development of a new preclinical model will facilitate molecular investigations on GO and evaluation of new therapeutic interventions. (*Endocrinology* 154: 3008–3015, 2013)

Graves' disease (GD) is an antibody-mediated autoimmune condition targeting the TSH receptor (TSHR) in the thyroid gland resulting in hyperthyroidism (1). Antibodies to TSHR modulate thyroid function and are responsible for GD, with thyroid stimulating antibodies (TSAbs) and TSH stimulating blocking antibodies (TSBAbs), which stimulate or inhibit TSHR signaling, respectively. Antibodies to TSHR with neutral properties are also present, which may also induce receptor signaling (2). A complication of GD is the extrathyroidal condition of

ISSN Print 0013-7227 ISSN Online 1945-7170
Printed in U.S.A.

Received June 22, 2013. Accepted July 17, 2013.
First Published Online July 30, 2013

For editorial see page 2989

Abbreviations: GD, Graves disease; GO, Graves' orbitopathy; H&E, hematoxylin-eosin; IGF-1R, IGF-1 receptor; IHC, immunohistochemistry; MRI, magnetic nuclear resonance; TSAbs, thyroid stimulating antibodies; TSBAbs, TSH stimulating blocking antibodies; TSHR, TSH receptor.

inflammatory eye disease known as Graves' orbitopathy (GO) (3). The inflammation in GO is characterized by orbital muscle inflammation and adipogenesis, resulting in expansion of the intraorbital tissue and proptosis (exophthalmos). Similar inflammation of eyelids leads to their swelling, redness, and edema (chemosis) (4). Whereas the pathogenic autoantigen in GD is undoubtedly TSHR, the role of autoimmunity to TSHR in GO remains uncertain (5). Other studies report IGF-1 receptor (IGF-1R) as a second pathogenic antigen in GO (6). Human orbital fibroblasts express TSHR and IGF-1R and a wealth of in vitro data support their role as important disease targets in GO (summarized in Ref. 5).

Molecular studies in GO on the role of TSHR and IGF-1R are hampered by the lack of a mouse model. Although a number of mouse models of GD have been developed (7), all singularly lack the complex pathology of orbital remodeling (7, 8). Accordingly, other reported mouse models of GO have proved difficult to replicate (9–11). In the course of our studies on experimental GD (12, 13), we recently expanded the human (h) TSHR A-subunit plasmid-in vivo electroporation model (14) to report histologic signs of orbital fibrosis in female BALB/c mice undergoing experimental hyperthyroidism (15). Upon observing orbital fibrosis, we modified our protocol to develop an improved mouse model with all the features of orbital inflammation, adipogenesis, and eyelid chemosis. Our findings in the new model raise novel issues on the role of autoimmune hypothyroidism and TSBAbs in the pathogenesis of GO.

Materials and Methods

The expression plasmids pTriEx-1.1 neo-hTSHR A-subunit, pTRiEx1.1 neo-IGF-1Rα, and pTRiEx1.1 neo-β-Gal plasmids have been described elsewhere (15). For immunization, female BALB/c mice were anesthetized for injection with 50 μL plasmid (1 mg/mL) into each biceps femoris (thigh) muscle (15). A single injection with the needle entered deep (3–4 mm) into the thigh muscle was performed, with slow release of plasmid into the muscle. Great care was taken to ensure reproducibility of the injection protocol in all immunizations. Injection and in vivo electroporation was performed 4 times at 3-week intervals using an ECM830 square wave electroporator with 7-mm caliper electrodes at 200 V/cm. Application of the current was in ten-20 millisecond square wave pulses at 1 Hz. All animals were maintained in conventional "clean" rooms and procedures were conducted under UK Government Home Office regulations of accepted standards of humane animal care.

Thyroid gland histology and orbital histology were conducted as described (11, 12, 16). All serum determinations were in individual mice for T4, anti-TSHR antibodies, and their subtypes, TSAbs and TSBAbs (13, 15). Antibodies to IGF-1R were evaluated by ELISA (17). In vivo magnetic nuclear resonance (MRI) was performed in immune (n = 5) and age-matched control mice (n = 3) on a horizontal bore 7T MRI scanner (Agilent Technologies, Inc, Palo Alto, California) and T2-weighted MRI images were acquired of the eyes and frontal region of the brain in anesthetized animals. Subsequently, t24 contiguous 0.4-mm thick, 94-μm in-plane resolution MR images were collected from the surface of the eye toward the back of the eye (perpendicular to the long axis of the eye, similar to the orientation for histologic processing. ImageJ (NIH) was used to view the MR images as well as measurement of the volume of the orbital muscle of the right eye.

Full methods are available in Supplemental Data published on The Endocrine Society's Journals Online web site at http://endo.endojournals.org. in the online version of the manuscript.

Results and Discussion

In this study, a total of 22 female BALB/c mice were immunized by the modified procedure with pTRiEx1.1 neo-hTSHR A-subunit plasmid and 12 animals were immunized with control plasmids.

hTSHR A-subunit plasmid-immunized mice are predominantly hypothyroid and show retrobulbar inflammation of extraocular muscles, adipogenesis, and chemosis

We initially challenged 8 mice with hTSHR A-subunit plasmid by the modified protocol. Animals were weighed weekly before the start of the immunization. Animals similarly immunized with pTRiEx1.1 neo-IGF-1Rα (n = 3) and pTRiEx1.1 neo-β-Gal plasmids (n = 3) did not lead to any visible changes in their health or to any histologic manifestations in thyroid and orbital tissue and were used as the control group. During the course of immunization, one animal showed severe signs of sickness 1 week after the third injection and was humanely destroyed. The finding of severe sickness prompted us to initially examine thyroid histology, which by hematoxylin-eosin (H&E) staining showed typical pattern of hypothyroidism, with most follicles characterized by thinning of epithelial cells (Figure 1A). The remaining 7 animals in the group were humanely destroyed 6 weeks after the end of immunization. H&E examination of thyroid glands identified 6 animals with typical features of hypothyroid glands. Inter-

estingly, one thyroid gland presented with hyperthyroid features characterized by hypertrophy and hypercellularity of the follicular epithelial cells (Figure 1B). There were no signs of thyroid inflammation (thyroiditis) in hTSHR A-subunit-immunized animals. Control thyroid glands showed normal appearance (Figure 1C).

We next examined the orbital tissues by H&E. Control mice showed normal appearance of orbital tissue (Figure 1D). Animals immunized with hTSHR A-subunit plasmid showed histologic signs of orbital pathology, with asymmetric bilateral disease. Two subtypes of orbital pathology were recognized: 1) interstitial inflammatory infiltrate into extraocular muscle, extending into the muscle tissue and isolating individual fibers (Figure 1E), observed bilaterally in 6 immune animals. Importantly, one animal (destroyed early due to severe sickness) showed a large inflammatory infiltrate around the optic nerve, revealing dense perineural inflammatory infiltrate, along with intense intermuscular lymphocytic infiltrate dissecting the orbital muscle fiber bundles (Figure 1, F and G), similar to that described in patients with active GO (18); and 2) orbital pathology developed by one animal with extensive adipogenesis, characterized by expansion of retrobulbar adipose tissue and widely separating the orbital muscle fiber bundles (Fig. l, H and I). By immunohistochemistry (IHC), the inflammatory cells were identified as CD3+ T cells and F4/80 + macrophages (Figure 1, J–L); the infiltrate was uniformly negative for B cells using antimouse B220 mAb (data not shown). Finally, one animal showed extraorbital changes with typical signs of acute orbital

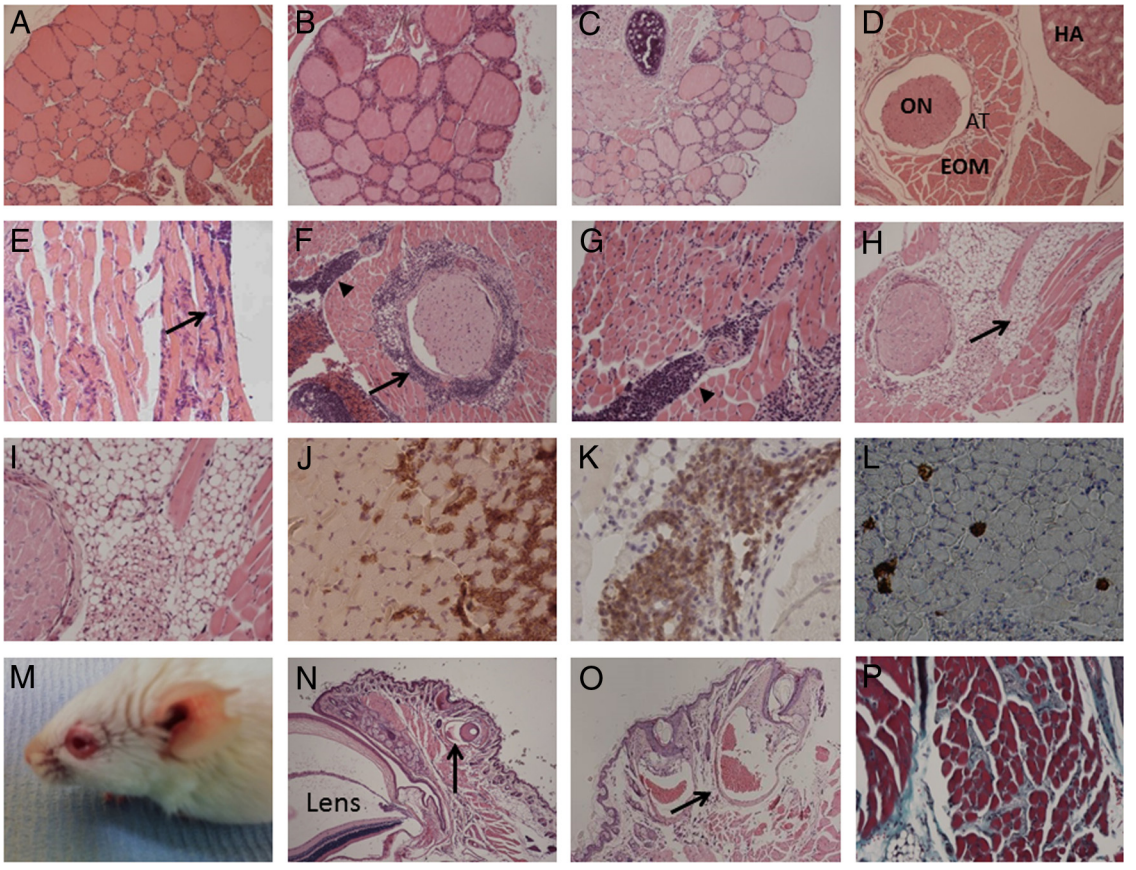

Figure 1. Histologic Features (H&E) of Thyroid Gland from hTSHR A-Subunit Plasmid Immunized Mouse Undergoing GO. A, Representative hypothyroid gland, magnification (×100); B, hyperthyroid gland (×200); C, thyroid gland from control mouse immunized with β-Gal plasmid (×100). H&E staining and IHC of orbital tissue, by orienting the paraffin block for sectioning, with optic nerve as an anatomic landmark. H&E stained sections from (D) orbit from control β-Gal plasmid-immunized mouse (×100) HA, harderian gland; ON, optic nerve; AT, adipose tissue; EOM, extraocular muscle. E, Representative extraocular muscle from hTSHR-A subunit plasmid-immunized mice (×200) showing interstitial inflammatory infiltrate (arrowed). F, optic nerve revealing dense perineural inflammatory infiltrate (arrowed), along with intense intermuscular lymphocytic infiltrate (arrowhead) (×100). G, Higher magnification (×200) to show the infiltrate dissecting the orbital muscle fiber bundles (arrowhead). H, Expansion of adipose tissue in retrobulbar fat (arrowed) (×100). I, Higher magnification (×200x) to show adipose tissue widely separating the orbital muscle fiber bundles. IHC to identify CD3+ T cells and F4/80+ macrophages in (J, ×400) serial section from panel E showing CD3+ T cells (stained in brown using 3,3′-diaminobenzidine as chromogen) infiltrating into the orbital muscle tissue. K, Serial section from panel F showing massive CD3+ T cells infiltrate surrounding the optic nerve (×400). L, F4/80+ macrophages in orbital muscle (×400). M, Appearance of head region of hTSHR-A subunit plasmid-immunized mouse undergoing chemosis. N, H&E-stained section of eye lid (×40) to show dilated and congested orbital blood vessels (arrowed), the lens is labeled; O, Higher magnification (×100) to show congested blood vessels (arrowed). P, Masson's Trichrome-stained section of orbital muscle (×200) to show pericellular fibrosis in retrobulbar tissue (15 weeks after end of immunization).

congestion (chemosis) (Figure 1M). Histologic examination of the eyelid showed dilated and congested orbital blood vessels with typical features of vascular inflammatory reaction (Figure 1, N and O).

We evaluated thyroid function and anti-TSHR antibodies in the above animals undergoing GO in serum obtained 6 weeks after end of immunization. Total T_4 measurements in mice undergoing experimental thyroid autoimmunity are hugely variable and not the most reliable indicators of thyroid function, but are commonly used for first assessment of endocrine status during the course of disease (13, 19, 20). Two animals showed significant depressed values of T_4, with remaining 5 mice showing a trend toward lower T_4 values, correlating with the findings of hypothyroid glands by histology (Figure 2A). The one animal with hyperthyroid histology showed significantly elevated levels of T_4. Importantly, the animals in the group showed significant weight gain during the course of immunizations, conferring hypothyroid status (Figure 2B). All animals showed high levels of antibodies to TSHR (Figure 2C). Determination of anti-TSHR antibody subtypes showed 3 animals highly positive for TSBAbs, ranging from 56 to 71% inhibition of TSH-mediated stimulation (Figure 2D). On the contrary, TSAb responses were modest ranging from 2–15 pmol/mL cAMP stimulation, compared with bovine (b)TSH (0.8 mU/mL) response of 570 pmol/mL cAMP in the assay (data not shown). Assessment of antibodies to IGF-1R by ELISA showed 6 animals with significantly positive antibodies, but the antibody titers are much lower than those from mice immunized with IGF-1Rα plasmids (Figure 2E).

Longitudinal studies on TSHR antibodies in mice undergoing GO and MRI of the orbital region

We performed longitudinal studies to evaluate TSHR antibodies in a new cohort of 8 female BALB/c mice challenged with TSHR A-subunit plasmid-in vivo electroporation. Serum was analyzed from weekly serial bleeds. This new group also served to evaluate the reproducibility of the model. In addition, in week 7 after the end of immunization, some immune animals underwent MRI (see below). All animals were humanely destroyed 9 weeks after end of immunization. Serum T_4 measurements showed 3 animals to be hypothyroid with significantly depressed hormone levels and 2 animals with elevated serum T_4 levels and thus hyperthyroid, (Figure 2A). High levels of anti-TSHR antibodies were present (Figure 2C), and comprised predominantly TSBAbs, which evolved early during the immune response and persisted for several weeks (Supplemental Figure 1A). A few animals were positive for TSAbs (Supplemental Figure 1B). Histologic analysis of thyroid glands showed 5 of 8 mice with hypothyroid glands (data not shown). Histologic analysis of the orbital tissue in this group showed the same pattern of orbital pathology as described for the 6 weeks after end of immunization group, comprising predominantly interstitial inflammatory infiltrate into extraocular muscle (data not shown). Importantly, disease heterogeneity was apparent by histologic analysis of the orbital tissue, with one animal with expansion of adipose tissue (Supplemental Figure 2B) and 2 animals with visible chemosis (Supplemental Figure 2. D and E). Histologic analysis of the latter animals confirmed dilated blood vessels with accompanying edema (Supplemental Figure 2, F and G). Interestingly, mast cells were readily recognized by morphology (Supplemental Figure 2H).

The extraocular muscles of 5 of the 8 immune animals were examined by MRI and compared with the orbital region of age-matched control mice. By in vivo MRI, the orbital muscles have lower signal intensity than the adjacent harderian gland as well as the cerebrospinal fluid that surrounds the optic nerve (Figure 3, A and B). Clear orbital muscle hypertrophy was apparent in the immune animals (Figure 3A) compared with the age-matched controls (Figure 3B). The position of the imaging slices to image the eye specifically with respect to the head is shown in Supplemental Figure 3i. Measurement of orbital muscle volumes from the MR images confirmed significant enlargement of extraocular muscles compared with age-matched controls (Figure 3C). Importantly, coronal MR images of the mouse head readily identified unilateral protrusion (proptosis) (Figure 3D), which was also apparent in another immune animal, but less pronounced (Figure 3E), compared with the control mouse (Figure 3F). The protrusion of the eye from the mouse head outline is clearly shown in Supplemental Fig 3ii. Unilateral protrusion had been apparent on visual inspection of the immune animals but was readily confirmed by in vivo MRI.

Long-term immunity to hTSHR leads to fibrosis of orbital muscle tissue

The hTSHR A-subunit plasmid-in vivo electroporation model in female BALB/c mice is recognized for robust antibody responses to TSHR, which persist for months after end of immunization (14, 15). The model therefore gave us the opportunity to evaluate the long-term effect of ongoing anti-TSHR immune response on orbital pathology. A group of 6 animals were immunized by the described protocol and tissue histopathology examined 15 weeks after end of immunization. Other animals were similarly immunized with control plasmids. Antibodies to TSHR persisted for 15 weeks (Figure 2C), with 4 of the 6 animals with strong TSBAb antibodies with weak TSAbs (data not shown). H&E examination of orbital tissue was charac-

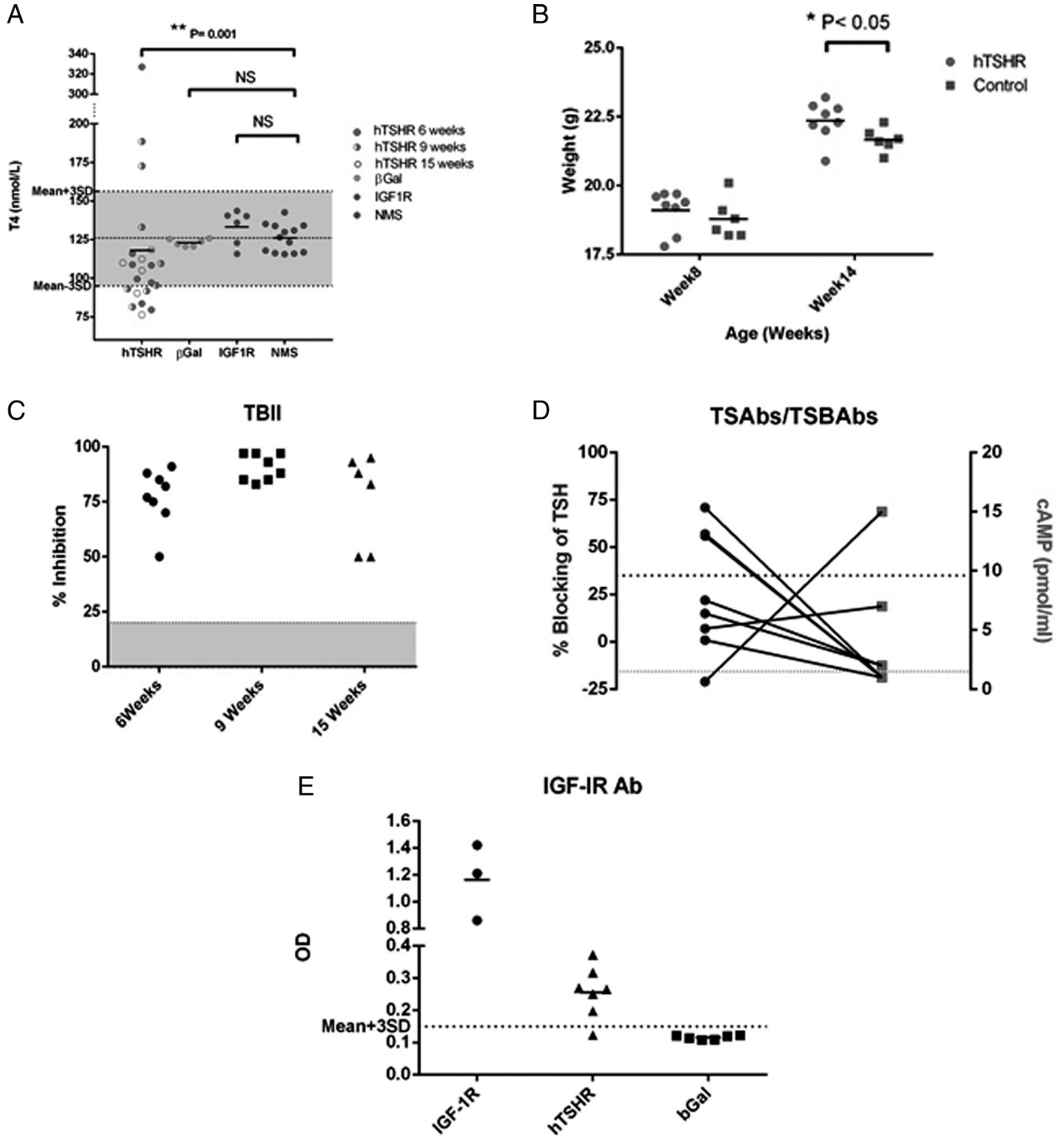

Figure 2. Evaluation of Thyroid Function and Antibody in TSHR A-Subunit Plasmid-Immunized Animals. A, Total serum T_4 values in blood obtained from mice undergoing experimental GO, killed at 6, 9, and 15 weeks after end of immunization. Also shown, T_4 values in mice similarly immunized with pTRiEx1.1 neo-IGF-1Rα plasmid (labeled IGF1) and pTRiEx1.1 neo-β-Gal plasmids-in vivo electroporation (labeled β-Gal) and serum from normal female BALB/c mice (labeled NMS). T_4 values in normal female BALB/c serum (age 12–14 weeks) are shown for comparison. ● = 6 weeks after end of immunization (labeled hTSHR 6 weeks); ◑ = 9 weeks after end of immunization (labeled hTSHR 9 weeks); ○ = 15 weeks after end of immunization (labeled hTSHR 15 weeks). B, Significant weight gain by mice during the course of immunization with pTRiEx1.1 hTSHR A-subunit plasmid (●) (labeled hTSHR) compared with combined group immunized with pTRiEx1.1 neo-IGF-1Rα plasmid and pTRiEx1.1 neo-β-Gal plasmid-in vivo electroporation (■) (labeled control). C, Measurement of total anti-TSHR antibodies in serum by TSH binding inhibitory immunoglobulin activity by competition with [^{125}I]bTSH. The abscissa shows serum values from mice killed after 6, 9 and 15 weeks after end of immunization, the ordinate refers to percent inhibition of [^{125}I]bTSH binding. The area between 0% and 15% represents the "gray" zone and values above this are generally scored positive. D, Measurements of blocking TSBAbs and stimulating TSAbs in individual animals by bioassay in the group of eight mice killed 6 weeks after end of immunization. The ordinate shows percent blocking of TSH-mediated stimulation for TSBAbs (left axis) or cAMP generated for TSAbs (right axis). The upper doted line and the grey lower line indicate the cut off for TSBAbs or TSAbs, respectively. E, Antibodies to IGF-1R by ELISA in mice immunized with hTSHR A-subunit plasmid, 6 weeks after end of immunization (labeled hTSHR), IGF-1Rα plasmid (labeled IGF-1R) and control β-Gal plasmid (labeled b-Gal). The dotted line indicates mean +3 SD for control β-Gal plasmid-immunized mice.

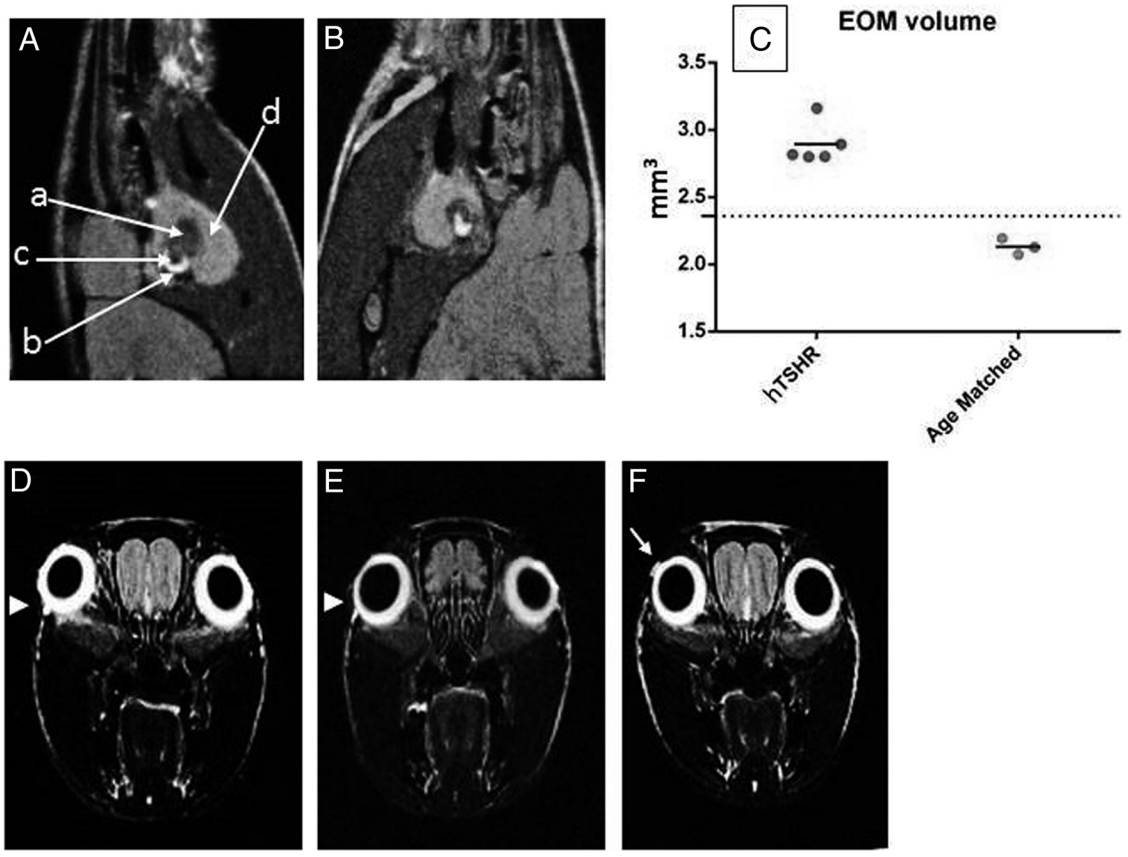

Figure 3. Typical in Vivo MR Images from an Immune (A) and Age-Matched Control (B) Female BALB/c Mouse Showing the Orbital Muscles. The orientation of the imaging slices is perpendicular to the longitudinal axis of the optic nerve as shown in Supplemental Figure 3i. The orbital muscles (labeled a) are of lower signal intensity than the adjacent cerebrospinal fluid (in white, labeled b) which encloses the optic nerve (labeled c). In turn, the orbital muscles are surrounded by the higher signal intensity of the harderian gland (labeled d). C, Hypertrophy of the orbital muscles shown as EOM volume in mm^3 (abscissa) in the immune mice compared with age-matched control mice. The hypertrophy was confirmed by segmentation analysis (Supplemental Figure 3i). D, Frontal in vivo MRI analysis of mouse head of immune animal to show protrusion (proptosis) of the right eye (highlighted by a white arrowhead) that is readily apparent in the coronal T2-weighted compared with the corresponding left eye. E, Second immune animal with less pronounced protrusion of the right eye (compared with D) (highlighted by a white arrowhead). F, Compared with age-matched control mice that show a lack of eye protrusion from the surface of the head region. The head outline is defined by the high-signal intensity of sc fat (arrow).

terized predominantly by orbital muscle fibrosis, which by Masson's Trichrome staining exhibited extensive deposition of glycosaminoglycans with pericellular fibrosis in retrobulbar tissue (Figure 1P). Interestingly, histologic analysis of the orbital tissue also showed disease heterogeneity in this group with one animal with expansion of adipose tissue (Supplemental Figure 2C) and one animal with a large inflammatory infiltrate around the optic nerve (Supplemental Figure 2A). Thyroid gland histology from 5 of the 6 animals showed hypothyroid status (data not shown).

In summary, all the total 22 immune animals show bilateral orbital pathology, as summarized in Supplemental Table 1. Unilateral protrusion was apparent in 2 immune animals and readily confirmed by in vivo MRI (Figure 3, D and E) (from 5 immune mice evaluated by MRI) compared with age-matched control mouse (Figure 3F). There was no correlation with subtype of GO pathology or onset of chemosis with thyroid status or presence and subtype of anti-TSHR (or IGF-1R) antibody in the model. None of the 12 animals immunized with control plasmids show any orbital pathology or disease.

Compared with our earlier study (15), it is not immediately apparent how the small modification of plasmid delivery resulted in marked different outcome in orbital pathology in the new model described herein. The small modifications to the delivery of hTSHR A-subunit plasmid involved a deeper injection of the plasmid over a larger muscle area, on the basis that this may lead to greater transfection efficiency during electroporation, resulting in alteration of antigenic stimulus and outcome of the anti-TSHR response (21, 22). In contrast to our previous findings (15), the small modification of plasmid delivery resulted in a marked different outcome in the immune response and consequent thyroid function, as well as the resultant orbital pathology. Both the earlier study (15) and the first group described in this report evaluated the im-

mune animals at 6 weeks after end of immunization, but with contrasting results. Thus, hyperthyroidism was induced in 8 of 12 immune animals (75%) in the former study, compared with 1 of 8 immune animals (12.5%) with hyperthyroidism after the modified immunization protocol in this study. Moreover, the modified protocol induced dramatic remodeling of the orbital region. The different pathologic, immunologic, and thyroid function outcomes in the model described in this study are not due neither to a change in the commercial supplier of the mice nor in the rodent chow diet (15). The animal unit housing conventional clean rooms also remained unchanged. The unit is tested quarterly for a wide range of pathogens, with no new or opportunistic infections reported. Thus, we conclude that a small modification in the injection delivery of the plasmid from that described previously (15) resulted in a dramatic different outcome in the immune response to TSHR (21, 22) with resultant orbital pathology.

Presently, the adenovirus model with hTSHR A-subunit immunization in female BALB/c mice is the most widely used experimental model of GD (7, 8), due to its high disease incidence and reproducibility in different laboratories, irrespective of housing in germ-free or conventional 'clean' rooms (13, 19, 20). Although this is an outstanding model for autoimmune thyroid hypertrophy, it does not lead to any orbital manifestations (8, 11, 19). There are a number of differences in the outcome of the anti-TSHR response between the adenovirus model and the plasmid-in vivo electroporation model described herein. Although both models are devoid of thyroid inflammation, the anti-TSHR responses in adenovirus model are dominated by hyperthyroidism and presence of TSAbs, which decline rapidly when the immunizations are terminated (13, 23). A surprising finding in the modified hTSHR A-subunit plasmid-in vivo electroporation model was the subtype of induced anti-TSHR antibodies, which were dominated by TSBAbs. Moreover, these evolved early during immunization and persisted for months. It can be postulated that these differences in the anti-TSHR response may contribute to the pathologic outcome in the 2 models. Recent findings from Nakahara and colleagues (24) provide some supportive evidence, in which they have expanded their studies by developing a unique authentic model of GD. The group used adenovirus coding for mouse (m) TSHR A-subunit for immunization of TSHR knockout mice, followed by adoptive transfer into immunodeficient mice (24). Although TSAbs and serum T_4 were transiently elevated in some animals, over time the antibodies switched to TSBAbs with consequent hypothyroidism. Notably, weak signs of orbital inflammation were manifest in a few animals (24). Thus, switching of the anti-TSHR response from TSAbs to TSBAbs (24, 25), or the dominant presence of TSBAbs and ensuring hypothyroidism during the course of autoimmunity as reported in this study, may be important contributory factors for onset of GO. However, there appear to be exceptions to this rule, because some animals in this study with predominantly TSAbs or neutral antibodies to TSHR also succumb to development of GO.

IGF-1R has been implicated in the pathogenesis and orbital remodeling in GO, with antibodies to IGF-1R being present in some GD patients undergoing GO (6), although the issue remains controversial (26). We found that immunization with IGF-1Rα plasmid-in vivo electroporation by the modified protocol gave results identical to those reported previously (15), with no apparent ill effects in the animals. However, using a well-established and reproducible ELISA (17), antibodies to IGF-1Rα-subunit were detectable in some animals immunized with TSHR A-subunit-in vivo electroporation, which may be related to the time when the serum was sampled after the end of immunization (Supplemental Table 1). However, because the anti-IGF-1R antibodies do not correlate with orbital pathology, further investigations will be necessary to gain clinical implications on the relationship between anti-TSHR and anti-IGF-1R antibodies induced by immunization with hTSHR A-subunit in the model.

Orbital imaging is often applied for diagnosis and response to treatment in patients with GO (27). It has been postulated that differences in the orbital bone structure between humans and rodents (16) may not allow manifestation of eyeball protrusion in the orbital region of mice (26). Despite this difference in orbital anatomy, we show by high-resolution in vivo MRI, clear hypertrophy of the orbital muscles and importantly, ready visualization of unilateral proptosis in some animals. B cells and germinal centers were not present in the inflammatory infiltrate in orbital region, similar to the findings in human orbital tissue (28). The antigen specificity of the inflammatory T cells in the orbital tissue of the immune animals requires investigation. In other studies, T cell lines generated from infiltrating retrobulbar tissue of GO patients have been characterized, but the antigen specificity was not investigated (28). Orbital fibroblasts are known to express high levels of functional TSHR (5), which is considered to be the target antigen for the inflammatory cells. If this was the case, then in the model described herein, it is interesting that the inflammatory T cells are recruited into the orbital tissue but do not infiltrate the thyroid gland with endogenous expression of TSHR. The specific targeting of the orbital tissue by inflammatory T cells may be related to the cytokines, possibly secreted by orbital fibroblasts or the adipose tissue. A better understanding of the inflammatory cytokines and the molecular pathways regulating endothelial migration of inflammatory cells into the orbital tissue, which bypass the thyroid gland, will lead to new knowledge

on orbital inflammation and potentially identify novel targets for therapeutic intervention. Recently, small molecule ligands (and monoclonal blocking antibodies) have been developed that act as antagonists for TSHR, which in in vitro studies show promise in blocking the signaling of the receptor (29, 30). The availability of a preclinical model that closely resembles the human condition will allow in vivo evaluation of these new therapeutic reagents for rapid translation to GO patients. In this context, the model also opens up new avenues to investigate the natural history of the condition, as well as the molecular basis of the effect of cigarette smoke on the condition.

Acknowledgments

We thank Professor Anja Eckstein (University of Duisberg-Essen, Germany) for the initial suggestion of using optic nerve as a landmark in orienting orbital tissue for histologic sectioning and guidance; Professor Miles Stanford (consultant ophthalmologist, KCH) for first identifying the onset of chemosis in the immune animals and for helpful discussions; Dr Michelle Ferrar in Department of Histopathology (KCH) for providing open access (to S.M.) to their modern equipment; Dr Mohamed Khalil (KCH) for advice and assistance on processing of orbital tissues; and Mr Adam Parkes (private affiliation) for photography of the immune animals.

Address all correspondence and requests for reprints to: J. Paul Banga, Division of Diabetes and Nutritional Sciences, King's College London School of Medicine, The Rayne Institute, 123 Coldharbour Lane, London, SE5 9NU, United Kingdom, E-mail: paul.banga@kcl.ac.uk.

The British Heart Foundation funded purchase of the MRI scanner in the Preclinical Imaging Unit, King's College London.

Disclosure Summary: The laboratory of J.P.B receives license income from ThermoFischer Scientific (Diagnostics). All other authors have nothing to disclose.

References

1. **Weetman AP.** Graves' disease. *New Engl J Med*. 2000;343:1236–1248.
2. **Morshed SA, Latif R, Davies TF.** Delineating the autoimmune mechanisms in Graves' disease. *Immunol Res*. 2012;54:191–203.
3. **Bahn RS.** Graves' ophthalmopathy. *N Engl J Med*. 2010;362:726–738.
4. **Dickinson AJ.** 2010 Clinical manifestation. In: Wiersinga WM, Kahaly GJ, eds. *Graves' Orbitopathy : A Multidisciplinary Approach—Questions And Answers*. 2nd rev. ed. Basel, Switzerland: S. Karger; 2010;1–25.
5. **Iyer S, Bahn R.** Immunopathogenesis of Graves' ophthalmopathy: the role of the TSH receptor. *Best Pract Res Clin Endocrinol Metab*.. 2012;26:281–289.
6. **Weightman DR, Perros P, Sherif IH, Kendall-Taylor P.** Autoantibodies to IGF-1 binding sites in thyroid associated ophthalmopathy. *Autoimmunity*. 1993;16:251–257.
7. **Dağdelen Su, Kong Y-C, Banga JP.** Toward better models of hyperthyroid Graves' disease. *Endocrinol Metab Clin North Am*. 2009;38:343–354.
8. **Wiesweg B, Johnson KT, Eckstein AK, Berchner-Pfannschmidt U.** Current insights into animal models of Graves' disease and orbitopathy. *Horm Metab Res*. 2013;45:549–555.
9. **Many MC, Costagliola S, Detrait M, Denef F, Vassart G, Ludgate MC.** Development of an animal model of autoimmune thyroid eye disease. *J Immunol*. 1999;162:4966–4974.
10. **Baker G, Mazziotti G, von Ruhland C, Ludgate M.** Reevaluating thyrotropin receptor-induced mouse models of graves' disease and ophthalmopathy. *Endocrinology*. 2005;146:835–844.
11. **Johnson KT, Wiesweg B, Schott M, et al.** Examination of orbital tissues in murine models of Graves' disease reveals expression of UCP-1 and the TSHR in retrobulbar adipose tissues. *Horm Metab Res*. 2013;45:401–407.
12. **Rao PV, Watson PF, Weetman AP, Carayanniotis G, Banga JP.** Contrasting activities of thyrotropin receptor antibodies in experimental models of Graves' disease induced by injection of transfected fibroblasts or deoxyribonucleic acid vaccination. *Endocrinology*. 2003;144:260–266.
13. **Gilbert JA, Gianoukakis AG, Salehi S, et al.** Monoclonal pathogenic antibodies to the thyroid-stimulating hormone receptor in Graves' disease with potent thyroid-stimulating activity but differential blocking activity activate multiple signaling pathways. *J Immunol*. 2006;176:5084–5092.
14. **Kaneda T, Honda A, Hakozaki A, Fuse T, Muto A, Yoshida T.** An improved Graves' disease model established by using in vivo electroporation exhibited long-term immunity to hyperthyroidism in BALB/c mice. *Endocrinology*. 2007;148:2335–2344.
15. **Zhao SX, Tsui S, Cheung A, Douglas RS, Smith TJ, Banga JP.** Orbital fibrosis in a mouse model of Graves' disease induced by genetic immunization of thyrotropin receptor cDNA. *J Endocrinol*. 2011;210:369–377.
16. **Smith RS.** *Systematic Evaluation of the Mouse Eye: Anatomy, Pathology, and Biomethods*. Boca Raton, LA; London, UK: CRC Press; 2002
17. **Yin KC, Chen D, Bakhtiar R, Verch T.** Evaluation of two ELISA methods to detect therapeutic anti-IGF1R antibodies in clinical study samples of dalotuzumab. *Bioanalysis*. 2011;3:2107–2117.
18. **Boschi A, Daumerie Ch, Spiritus M, et al.** Quantification of cells expressing the thyrotropin receptor in extraocular muscles in thyroid associated orbitopathy. *Br J Ophthalmol*. 2005;89:724–729.
19. **Nagayama Y, Kita-Furuyama M, Ando T, Nakao K, Mizuguchi H, Hayakawa T, Eguchi K, Niwa M.** A novel murine model of Graves' hyperthyroidism with intramuscular injection of adenovirus expressing the thyrotropin receptor. *J Immunol*. 2002;168:2789–2794.
20. **Chen CR, Pichurin P, Nagayama Y, Latrofa F, Rapoport B, McLachlan SM.** The thyrotropin receptor autoantigen in Graves disease is the culprit as well as the victim. *J Clin Invest*. 2003;111:1897–1904.
21. **Cemazar M, Golzio M, Sersa G, Rols MP, Teissie J.** Electrically-assisted nucleic acids delivery to tissues in vivo: where do we stand? *Curr Pharm Des*. 2006;12:3817–3825.
22. **Chen CR, Pichurin P, Chazenbalk GD, et al.** Low-dose immunization with adenovirus expressing the thyroid-stimulating hormone receptor A-subunit deviates the antibody response toward that of autoantibodies in human Graves' disease. *Endocrinology*. 2004;145:228–233.
23. **McLachlan SM, Aliesky HA, Chen CR, Rapoport B.** Role of self-tolerance and chronic stimulation in the long-term persistence of adenovirus-induced thyrotropin receptor antibodies in wild-type and transgenic mice. *Thyroid*. 2012; 22:931–937.
24. **Nakahara M, Johnson K, Eckstein A, et al.** Adoptive transfer of antithyrotropin receptor (TSHR) autoimmunity from TSHR knockout mice to athymic nude mice. *Endocrinology*. 2012;153:2034–2042.
25. **McLachlan SM, Rapoport B.** Thyrotropin-blocking autoantibodies and thyroid-stimulating autoantibodies: potential mechanisms involved in the pendulum swinging from hypothyroidism to hyperthyroidism or vice versa. *Thyroid*. 2013;23:14–24.
26. **Wiersinga WM.** Autoimmunity in Graves' ophthalmopathy: the result of an unfortunate marriage between TSH receptors and IGF-1 receptors? *J Clin Endocrinol Metab*. 2011;96:2386–2394.
27. **Müller-Forell W, Kahaly GJ.** Neuroimaging of Graves' orbitopathy. *Best Pract Res Clin Endocrinol Metab*. 2012;26:259–271.
28. **Grubeck-Loebenstein B, Trieb K, Sztankay A, Holter W, Anderl H, Wick G.** Retrobulbar T cells from patients with Graves' ophthalmopathy are CD8+ and specifically recognize autologous fibroblasts. *J Clin Invest*. 1994;93: 2738–2743.
29. **van Zeijl CJ, van Koppen CJ, Surovtseva OV, et al.** Complete inhibition of rhTSH-, Graves' Disease IgG-, and M22-Induced cAMP production in differentiated orbital fibroblasts by a low-molecular-weight TSHR antagonist. *J Clin Endocrinol Metab*. 2012;97:E781–E785.
30. **Turcu AF, Kumar S, Neumann S, et al.** A small molecule antagonist inhibits thyrotropin receptor antibody-induced orbital fibroblast functions involved in the pathogenesis of graves ophthalmopathy. *J Clin Endocrinol Metab*. 2013; 98:2153–2159.